Mössbauer and magnetization studies of Fe_2BO_4

2000 J. Phys.: Condens. Matter 12 177

(http://iopscience.iop.org/0953-8984/12/2/307)

J. Phys.: Condens. Matter **12** (2000) 177–188. Printed in the UK PII: S0953-8984(00)08402-2

Mössbauer and magnetization studies of Fe_2BO_4

A P Douvalis†, V Papaefthymiou†, A Moukarika†, T Bakas† and G Kallias‡

† Physics Department, University of Ioannina, PO Box 1186, 45 110 Ioannina, Greece
‡ Institute of Materials Science, National Centre for Scientific Research 'Demokritos', 153 10 Athens, Greece

Received 4 October 1999

Abstract. Polycrystalline Fe_2BO_4 prepared by solid-state reaction was investigated over a wide temperature range using Mössbauer spectroscopy and magnetization and resistivity measurements. The Mössbauer data below 270 K reveal four iron sites (two Fe^{2+} and two Fe^{3+}) in a 1:1:1:1 ratio. Above this temperature, electron delocalization sets in between the divalent–trivalent iron ions and up to 400 K both delocalized and localized iron states are observed. The magnetization and Mössbauer data indicate that this oxoborate mixed-valence system is an L-type ferrimagnet below $T_c = 155$ K, with the iron atoms in each sublattice having different point symmetries and different magnetic interactions. The resistivity data show the first-order nature of the charge-ordering transition ($T_{co} = 316$ K).

1. Introduction

The iron borate Fe_2BO_4 is a mixed-valence iron (Fe^{2+}–Fe^{3+}) oxide and belongs to a family of oxyborates with very interesting electronic and magnetic properties [1, 2]. Even though the crystal and magnetic structures of this phase have been examined by means of neutron diffraction [1], there is no report of detailed Mössbauer studies, mainly because of the difficulties in preparing samples without ferrimagnetic impurities which hinder the consistent analysis of the spectra. The crystal structure at 300 K has been found to differ from the originally reported orthorhombic warwickite structure at 300 K [3] by a monoclinic distortion [1, 3]. Recent studies [4, 5] have shown the occurrence of a monoclinic–orthorhombic structural transition at 317 K, with a concomitant charge delocalization above this temperature. Notably, the extent of the charge-ordered domains is small (10–100 Å) and no superstructure peaks were observed in diffraction experiments. In neutron diffraction experiments magnetic peaks were observed below 160 K and the magnetic structure was found to be commensurate with the crystal one. The moments at the two Fe sites (M1 and M2) are antiparallel but the inequivalence of the two sublattices results in an L-type ferrimagnetic order, which in the present work was determined by both Mössbauer spectroscopy and SQUID magnetometry to occur at 155 ± 1 K.

In the present work, we report detailed Mössbauer measurements in the temperature range 4.2 to 650 K. The analysis of the spectra reveals the existence of spin clusters close to T_c, and above 270 K charge delocalization among the mixed-valence iron pairs. The magnetic ($T_c = 155$ K) and the charge-ordering transitions ($T_{co} = 316$ K) were determined by magnetization and resistivity measurements, respectively.

0953-8984/00/020177+12$30.00

2. Experimental procedure

Polycrystalline powder of Fe_2BO_4 was prepared by solid-state reactions. Heat treatment, at 800 °C for 25 h, of stoichiometric amounts of $FeBO_3$, α-Fe and α-Fe_2O_3, in an evacuated quartz tube, gave pure Fe_2BO_4. Mössbauer spectra with high statistics gave an upper limit of 0.2% for the iron oxides Fe_3O_4 and α-Fe_2O_3.

The x-ray diffraction pattern at room temperature (RT) was taken in the Bragg–Brentano geometry (from 10–80° with a step of 0.03°) with Cu Kα radiation using a graphite crystal monochromator (Siemens D500). The Rietveld profile analysis [6] revealed single-phase material with the refined values of the unit-cell parameters at 300 K close to those reported by Attfield *et al* [4, 5]. The refined XRD pattern is shown in figure 1 and the refined parameters are listed in table 1.

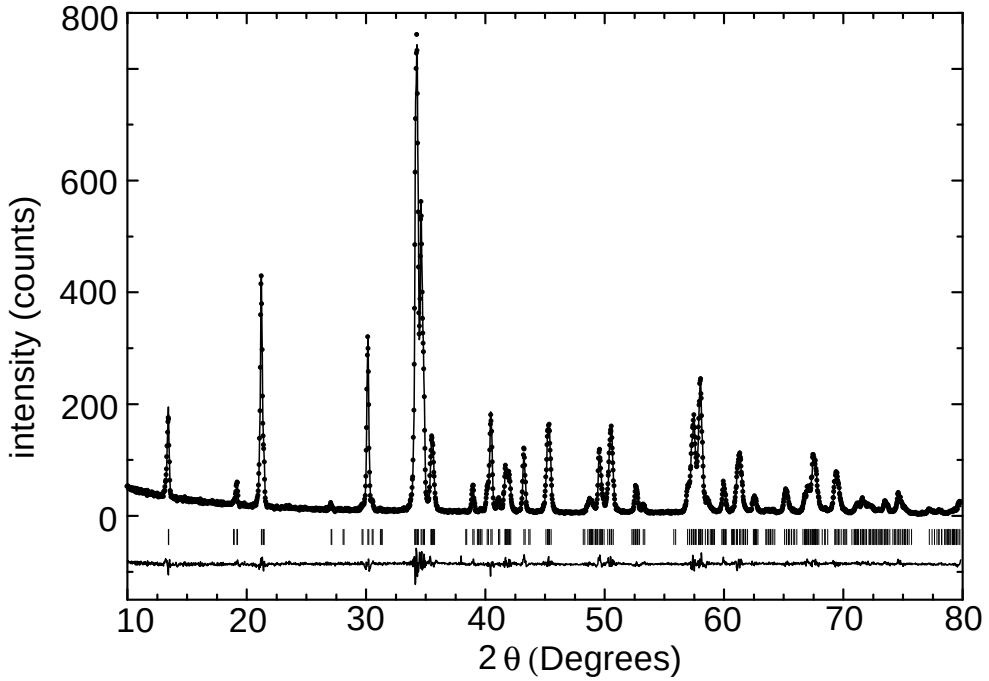

Figure 1. The Rietveld refinement pattern for powder x-ray diffraction data for Fe_2BO_4 at RT. The observed intensities are shown by crosses and the calculated ones by the solid lines. The positions of the Bragg reflections are shown by the small vertical lines below the pattern. The line at the bottom indicates the intensity difference between the experimental and refined patterns.

Mössbauer measurements were carried out using a constant-acceleration Mössbauer system with a ^{57}Co(Rh) source maintained at room temperature. A closed-loop He system (Air Products) and a variable-temperature liquid-nitrogen/helium cryostat (Oxford Instruments) were used for low-temperature measurements and a Mössbauer vacuum furnace was used for measurements above RT. All isomer shifts are quoted relative to that of iron metal at RT. The bulk magnetic susceptibility measurements were performed using a SQUID magnetometer (Quantum Design) in the temperature range 4.2–350 K. Four-probe resistivity measurements with and without a magnetic field were performed on a sintered bar of Fe_2BO_4 from 350 to 200 K (below which the extremely large resistance of the sample precluded accurate measurement).

Table 1. Refined fractional atomic positions, unit-cell parameters and reliability factors derived from x-ray diffraction data for Fe_2BO_4. The monoclinic space group $P2_1/c$ (No 14) was used. The various ions occupy the 4e (x, y, z) site. The numbers in the parentheses are the statistical errors of the last significant digit. ($a = 3.1759(2)$ Å, $b = 9.3811(5)$ Å, $c = 9.2428(5)$ Å, $\beta = 90.247(2)^\circ$, $R_p = 4.4$, $R_{wp} = 8.1$, $R_B = 2.79$.)

Atom	x	y	z
Fe(M1)	0.752(2)	0.0679(2)	0.1183(2)
Fe(M2)	0.248(1)	0.1944(2)	0.3985(2)
B	0.749(9)	0.381(2)	0.167(2)
O1	0.246(4)	0.1192(8)	−0.0091(6)
O2	0.752(5)	0.0093(8)	0.2682(8)
O3	0.737(5)	0.2533(7)	0.242(1)
O4	0.756(5)	0.3732(8)	0.0178(8)

3. Results and discussion

3.1. Susceptibility measurements

Figure 2 shows magnetic susceptibility measurements (χ versus T) in both zero-field (ZFC) and field-cooling (FC) modes for magnetic fields of 1 and 50 kOe. The ZFC curve at $H = 1$ kOe shows a sharp maximum just below $T_c = 155$ K. The corresponding curve in 50 kOe shows

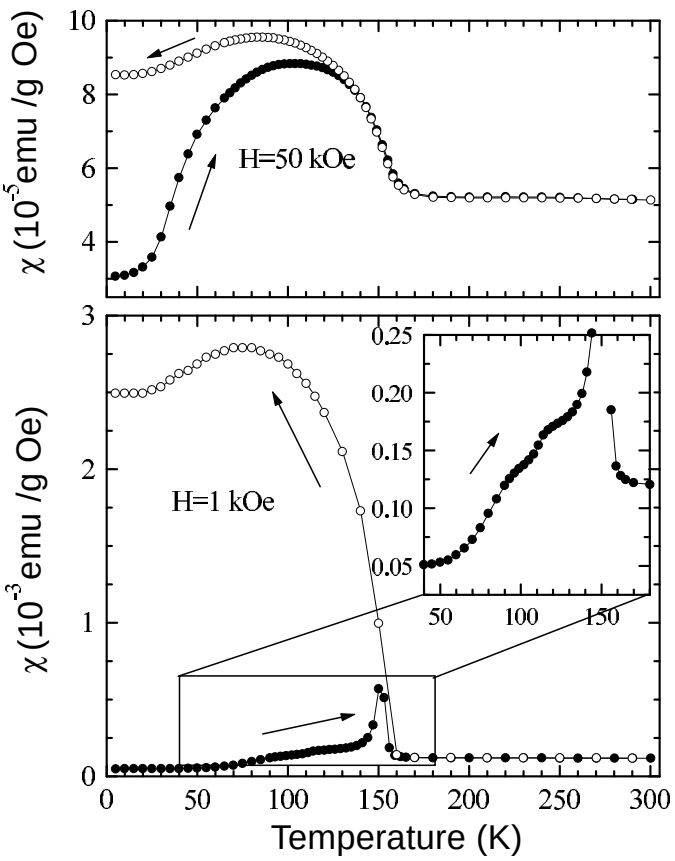

Figure 2. Magnetic susceptibility versus temperature in ZFC and FC modes of Fe_2BO_4 in applied magnetic fields of 1 and 50 kOe. The filled symbols represent the ZFC curves and the open ones are the FC ones. Inset: an expanded view of the ZFC curve at $H = 1$ kOe.

a broad maximum around 100 K and the transition is smeared out. Below T_c, for both fields the two branches (ZFC and FC) diverge. The maximum observed in the susceptibility around 80 K ($H = 1$ kOe) in the FC mode cannot be explained by solely antiferromagnetic ordering and is characteristic of L-type ferrimagnetic ordering in accordance with previous results [5]. The ferrimagnetic character is also reflected in the different temperature dependence of the hyperfine fields determined from the Mössbauer spectra (*vide infra*). A Curie–Weiss law $\chi = C/(T - \Theta_p)$ is followed in the range 200–300 K with a rather large negative value of Θ_p and a large constant C, unexpected from the free-ion Curie constants of the constituent ions. Note that the values of χ in this temperature range have magnitudes of 10^{-4} to 10^{-5} emu g^{-1} Oe^{-1}. This behaviour implies ferromagnetic pair correlations even in the paramagnetic state, above 155 K [7]. The susceptibility curve (see the inset in figure 2) shows three changes in the slope at around 120, 90 and 50 K, which could be attributed to the different temperature dependences of the magnetic moments in the two sublattices.

3.2. Resistivity measurements

Figure 3 shows the temperature dependence of the resistivity in a $\log \rho$ versus $1/T$ plot. Below 270 K the resistivity can be described by a thermally activated electron hopping law ($\rho = A \exp(-E_a/k_B T)$) with activation energy $E_a = 0.33$ eV. The charge-ordering transition (marked for clarity at the change in the slope of the variation in ρ versus T in the inset of figure 3) at $T_{co} = 316$ K clearly shows hysteresis, indicative of a first-order transition. In the vicinity of the charge-ordering transition the resistivity shows a rather complicated temperature variation.

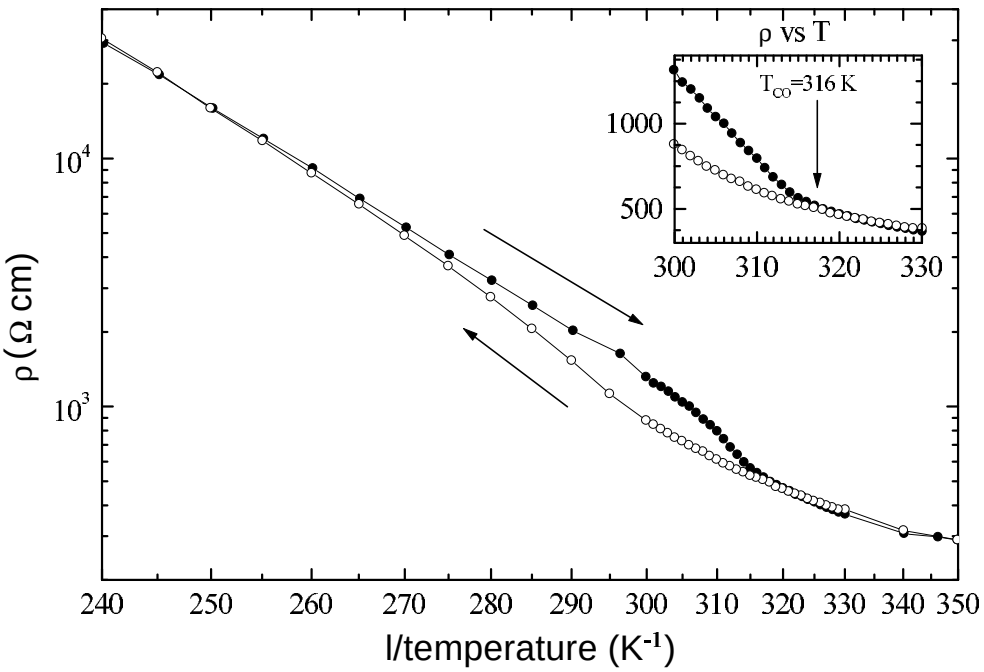

Figure 3. A plot of $\log \rho$ versus $1/T$ (with a descending $1/T$ scale with T indicated) for Fe_2BO_4. Inset: the variation of ρ versus T near the charge-ordering transition, which is marked by a change of slope at $T_{co} = 316$ K.

3.3. Mössbauer data

The Mössbauer spectra (MS) at all temperatures revealed that Fe_2BO_4 was the only Fe-containing phase. This is crucial for the analysis of the Mössbauer and magnetic susceptibility data. Representative MS from 4.2 up to 650 K are shown in figures 4, 5, 6 and 7. For $T < 155$ K we observed six-line MS due to magnetic interactions (magnetic order) and above $T_c = 155$ K paramagnetic spectra were observed. In the temperature region $155 < T < 270$ K the fitted parameters indicate localized Fe^{2+} and Fe^{3+} states. From 270 to 400 K delocalized (hyperfine parameters corresponding to $Fe^{2.5+}$) and localized Fe states coexist. Finally, above 400 K only the delocalized state is observed.

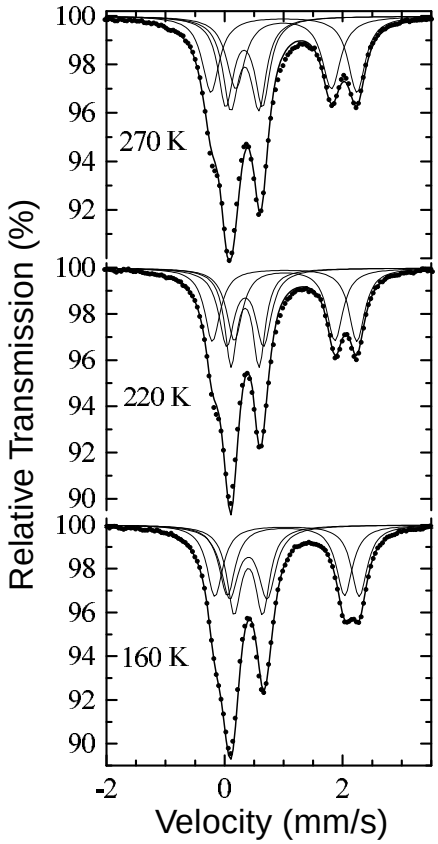

Figure 4. Mössbauer spectra recorded at temperatures between 160 and 270 K. The solid lines result from least-squares fits using Lorentzians (the parameters are shown in table 2).

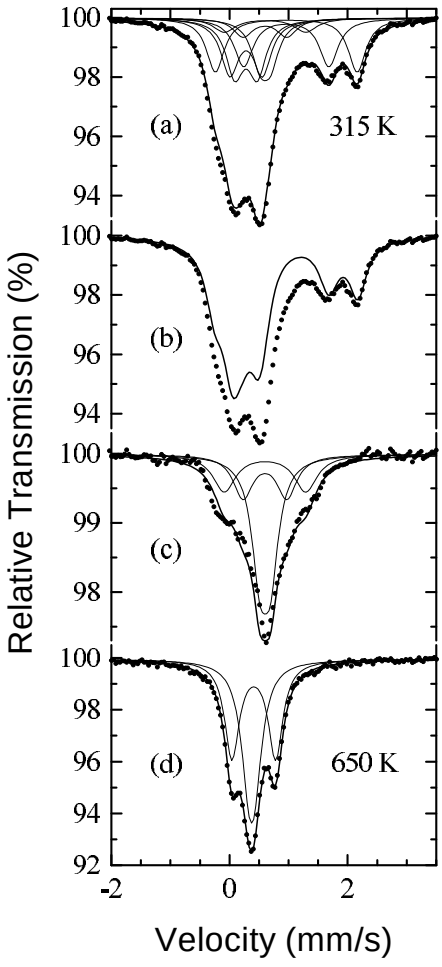

Figure 5. Mössbauer spectra at (a) 315 K and (b) 315 K with the solid line indicating the localized spectrum after appropriate scaling, (c) the difference spectrum of the two spectra shown in (b), and (d) that at 650 K. The solid lines in (a), (c) and (d) are the components used for the fitting of the spectra.

Table 2. Experimental values of the half-linewidth $\Gamma/2$ in mm s^{-1}, the isomer shift δ relative to that of α-Fe at RT in mm s^{-1} and the quadrupole shift ΔE_Q in mm s^{-1} as obtained from least-squares fits of the Mössbauer spectra of Fe_2BO_4 between 160 and 270 K. ΔE_Q denotes the eigenvalues of the Hamiltonian of the quadrupole interaction that are given by the relation $\Delta E_Q = (1/2)e^2qQ(1+\eta^2/3)^{1/2}$.

T (K)	Site	δ	ΔE_Q	$\Gamma/2$	Area (%)
160	Fe_b^{3+}	0.51	0.64	0.18	26
	Fe_a^{3+}	0.51	0.49	0.14	25
	Fe_a^{2+}	1.15	1.99	0.17	25
	Fe_b^{2+}	1.17	2.45	0.16	24
220	Fe_b^{3+}	0.46	0.63	0.18	26
	Fe_a^{3+}	0.46	0.48	0.14	25
	Fe_a^{2+}	1.13	1.70	0.17	25
	Fe_b^{2+}	1.13	2.45	0.16	24
270	Fe_b^{3+}	0.43	0.62	0.18	26
	Fe_a^{3+}	0.43	0.48	0.14	25
	Fe_a^{2+}	1.11	1.62	0.17	25
	Fe_b^{2+}	1.11	2.47	0.16	24

3.3.1. Mössbauer spectra for $T > T_c$. The MS recorded for $155 < T < 270$ K (figure 4) show well resolved absorption lines, while for $T > 270$ K (figures 5 and 6) broadened, more complex, quadrupole-split MS were obtained.

The MS in the temperature region $155 < T < 270$ K were analysed with four doublets. The fitting parameters are listed in table 2 and it is clear that two of the doublets can be assigned to high-spin, octahedrally oxygen-coordinated Fe^{2+}, while the other two doublets can be assigned to high-spin Fe^{3+} with the same oxygen coordination [8]. The area ratio of the four components is Fe_a^{2+}:Fe_b^{2+}:Fe_a^{3+}:Fe_b^{3+} = 1:1:1:1 and thus the Fe^{2+} and Fe^{3+} ions are evenly distributed among the M1 and M2 sites. This consistent equal occupancy throughout the above temperature range indicates equal Debye–Waller factors for all of the corresponding iron sites.

The quadrupole splitting values of the Fe_a^{2+} and Fe_b^{2+} are different, as are those of Fe_a^{3+} and Fe_b^{3+}. Also, the temperature variation of the quadrupole splitting of the Fe_a^{2+} is more pronounced than that of the Fe_b^{2+}. All of these results can be explained by the fact that the symmetry at one of the two crystallographic Fe sites is less distorted [9].

Above 270 K a four-component fit does not reproduce the spectra and above 340 K the spectral resolution is lost. For $T > 400$ K the spectra are again well resolved, consisting of three sharp lines, which can be fitted with two components. The isomer shift of these two components (table 3) is equal to the average value of the four components used below 270 K (corrected for second-order Doppler shift), indicating a delocalized intermediate-valence state, where the excess electron of Fe^{2+} is equally shared among the Fe^{2+} and Fe^{3+} sites. In other words, the valence of these delocalized states takes the formal value 2.5+ ('ferroic ions').

In the temperature range 270–400 K, as the temperature is raised, we observe a decrease of the rightmost absorption lines (characteristic of Fe^{2+} sites) and the spectral resolution in the middle of the spectrum is also decreased. In order to examine the evolution of the MS in the temperature region 270–400 K, we employed difference spectra. A difference spectrum was obtained by subtracting the four-doublet pattern at $T = 270$ K (figure 4) from the raw

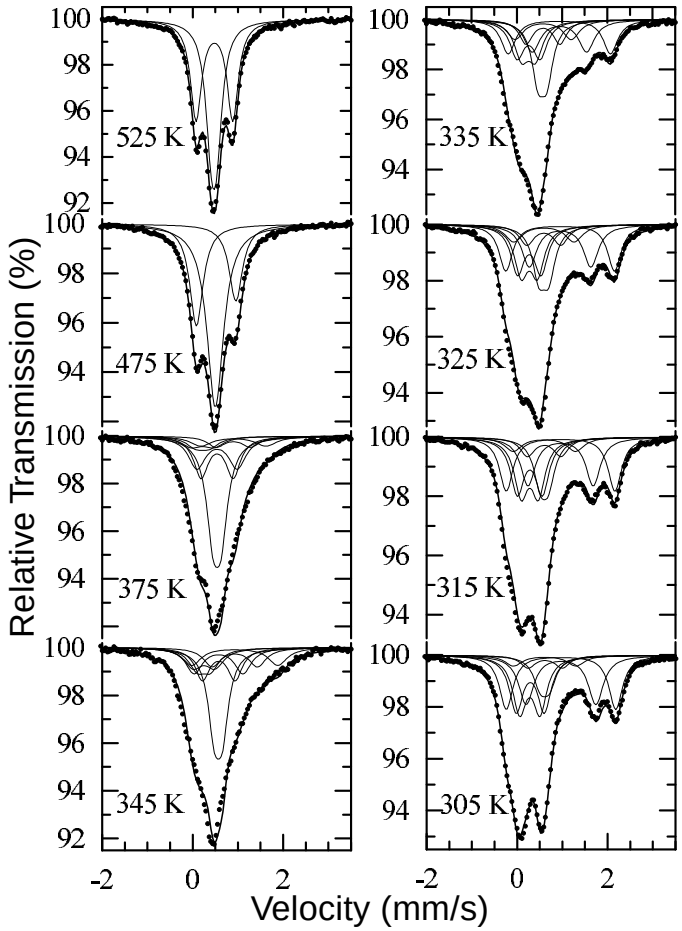

Figure 6. Representative Mössbauer spectra of Fe_2BO_4 at $T > 270$ K. The solid lines are least-squares fits as described in the text (the parameters are listed in table 3).

data at 315 K (figure 5(b)), after appropriate scaling. The difference spectrum (figure 5(c)) shows a profile very similar to the one that appeared at $T > 470$ K (figure 5(d)). As a result, the difference spectrum could be attributed to totally delocalized sites. An analysis of this difference spectrum with two doublets, like that at 650 K, with relative area ratio 1:1, did not give reasonable fits. More plausible fits were obtained with three doublets whose area ratio was 0.5:0.5:1. The isomer shift values of the three doublets are equal and fairly close to the weighted average of those for Fe^{2+} and Fe^{3+} with an octahedral oxygen environment. Therefore, in order to fit the MS taken in the temperature range 270–400 K we had to use four localized sites similar to those used at $T < 270$ K plus three additional doublets corresponding to three sites with totally delocalized charge (see table 3), as shown in figure 6. The isomer shift and quadrupole splitting values for the localized sites are typical for high-spin ferric and ferrous ions in octahedral coordination with oxygens. For the three delocalized sites the isomer shift values can be readily interpreted as arising from an iron $Fe^{2.5+}$ oxidation level with quadrupole splitting values intermediate between those of Fe^{2+} and Fe^{3+} in the same environment, but not equal to the average values which would be expected for equivalent sites in a totally delocalized

Table 3. Experimental values of the half-linewidth $\Gamma/2$ in mm s^{-1}, the isomer shift δ relative to that of α-Fe at RT in mm s^{-1} and the quadrupole shift ΔE_Q in mm s^{-1} as obtained from least-squares fits of the Mössbauer spectra of Fe_2BO_4 between 270 and 650 K. ΔE_Q denotes the eigenvalues of the Hamiltonian of the quadrupole interaction that are given by the relation $\Delta E_Q = (1/2)e^2qQ(1+\eta^2/3)^{1/2}$.

T (K)	Site	δ	ΔE_Q	$\Gamma/2$	Area (%)
305	Fe^{3+}	0.40	0.62	0.18	20
	Fe^{3+}	0.39	0.45	0.18	20
	Fe^{2+}	1.08	1.54	0.20	20
	Fe^{2+}	1.08	2.42	0.18	20
	$Fe^{2.5+}$	0.73	0.76	0.20	5
	$Fe^{2.5+}$	0.72	1.38	0.23	5
	$Fe^{2.5+}$	0.72	0.20	0.18	10
315	Fe^{3+}	0.39	0.55	0.18	19
	Fe^{3+}	0.39	0.38	0.18	19
	Fe^{2+}	1.07	1.44	0.19	18
	Fe^{2+}	1.07	2.40	0.18	18
	$Fe^{2.5+}$	0.71	0.74	0.20	7
	$Fe^{2.5+}$	0.71	1.38	0.23	6
	$Fe^{2.5+}$	0.71	0.18	0.18	13
325	Fe^{3+}	0.38	0.52	0.18	17
	Fe^{3+}	0.38	0.36	0.18	17
	Fe^{2+}	1.06	1.36	0.20	17
	Fe^{2+}	1.06	2.40	0.18	17
	$Fe^{2.5+}$	0.70	0.75	0.20	8
	$Fe^{2.5+}$	0.70	1.33	0.23	8
	$Fe^{2.5+}$	0.70	0.22	0.17	16
335	Fe^{3+}	0.37	0.51	0.19	15
	Fe^{3+}	0.37	0.31	0.19	15
	Fe^{2+}	1.05	1.20	0.21	15
	Fe^{2+}	1.05	2.26	0.19	15
	$Fe^{2.5+}$	0.69	0.75	0.18	10
	$Fe^{2.5+}$	0.69	1.24	0.22	10
	$Fe^{2.5+}$	0.68	0.20	0.17	20

Fe^{2+}–Fe^{3+} pair. This situation may arise from the fact that the electric field gradient (EFG) tensors in the mixed-valence pairs do not coincide and/or the site symmetries are different. Thus, the two iron sites of the delocalized pair are not equivalent from the quadrupole splitting point of view.

Some remarks regarding the temperature variation of the hyperfine parameters of the quadrupole doublets are of interest here. The temperature variation of the isomer shift values is linear as expected from the second-order Doppler-shift effect. The quadrupole splitting values of the localized sites display an abrupt decrease at about 320 K which is consistent with the monoclinic-to-orthorhombic structural phase transition at 317 K [4, 5]. It is interesting to note that delocalization appears close to this temperature. We may thus assume that these two phenomena are interconnected.

To summarize the unusual temperature variation of the MS in the paramagnetic regime, below 270 K the charges are localized resulting in two Fe^{2+} and two Fe^{3+} ions equally distributed at the M1 and M2 crystallographic sites, and above 270 K charge delocalization

Table 3. (Continued)

T (K)	Site	δ	ΔE_Q	$\Gamma/2$	Area (%)
345	Fe^{3+}	0.36	0.48	0.24	11
	Fe^{3+}	0.36	0.30	0.22	10
	Fe^{2+}	1.04	1.00	0.23	10
	Fe^{2+}	1.04	1.90	0.25	11
	$Fe^{2.5+}$	0.68	0.72	0.18	15
	$Fe^{2.5+}$	0.68	1.08	0.22	14
	$Fe^{2.5+}$	0.68	0.18	0.18	29
375	Fe^{3+}	0.33	0.50	0.27	6
	Fe^{3+}	0.33	0.30	0.25	7
	Fe^{2+}	1.01	0.76	0.23	6
	Fe^{2+}	1.01	1.44	0.29	7
	$Fe^{2.5+}$	0.65	0.71	0.19	19
	$Fe^{2.5+}$	0.65	0.89	0.23	18
	$Fe^{2.5+}$	0.65	0.18	0.18	37
475	$Fe^{2.5+}$	0.61	0.85	0.19	50
	$Fe^{2.5+}$	0.61	0.18	0.18	50
525	$Fe^{2.5+}$	0.59	0.81	0.15	50
	$Fe^{2.5+}$	0.58	0.12	0.15	50
650	$Fe^{2.5+}$	0.50	0.74	0.15	50
	$Fe^{2.5+}$	0.49	0.12	0.15	50

starts between Fe^{2+} and Fe^{3+} ions producing intermediate-valence states and charge disorder. The delocalization process is completed at about 400 K; however, in this temperature range localized and delocalized states coexist. The localization–delocalization transition in the temperature range 270–400 K might be associated with the crystallographic transition observed at $T = 316$ K.

3.3.2. Mössbauer spectra for $T < T_c$. Representative magnetically split spectra are shown in figure 7. Below 110 K the absorption lines are sharp and the shape of the MS is typical for a multicomponent well resolved Zeeman-split spectrum. Above 110 K the MS show broad lines and substantial absorption around zero velocity, which implies that these spectra comprise magnetic as well as paramagnetic components, whose area increases as the temperature is raised.

Starting at lower temperatures, where only magnetic hyperfine splitting is observed, we employed four Zeeman-split components (sextets) with Lorentzian line shapes. Following the analysis of the paramagnetic spectra in the charge-localized regime, the area ratio of the four magnetic components was 1:1:1:1. The initial isomer shift and quadrupole splitting values for these magnetic components were deduced from those of the paramagnetic spectra with the appropriate correction for second-order Doppler shift. This fitting scheme gave adequate χ^2-fits and consistent hyperfine parameters. Representative fitted MS at 26 and 80 K are shown in figure 7 and the fitted parameters are listed in table 4.

From the values of the hyperfine parameters in tables 2 and 4, we can conclude that for $T < 110$ K, the magnetic components can be directly assigned to the paramagnetic components observed above 155 K, corresponding to two Fe^{2+} and two Fe^{3+} sites.

Above 120 K a paramagnetic central feature appears, which dominates the spectrum as we

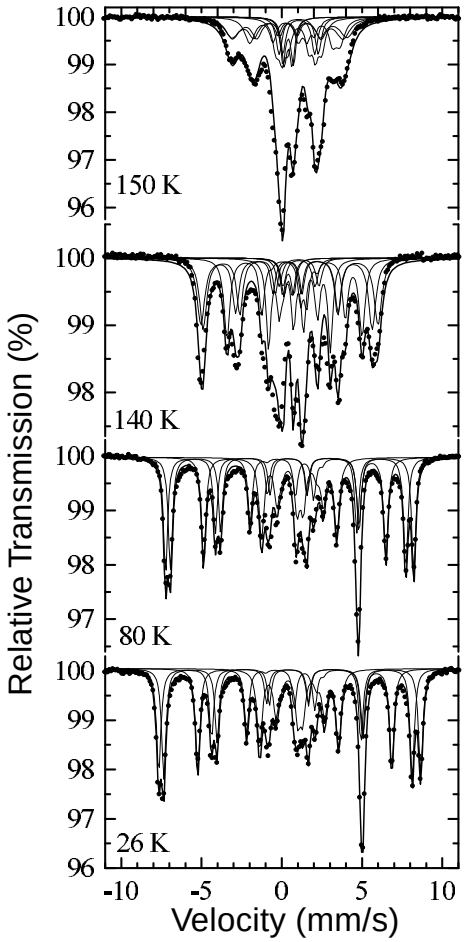

Figure 7. Representative Mössbauer spectra for $T < 155$ K. The solid lines are theoretical curves computed with the parameters of table 4.

approach T_c. This is untypical behaviour for an isotropic magnetically ordered system where the MS below the transition temperature consist only of sextets with narrow Lorentzian lines. The observed temperature evolution of the magnetic MS and the coexistence of magnetic and paramagnetic components as we approach T_c have been observed in several studies [10–14].

Line broadening of the MS in magnetically ordered systems in this temperature regime may occur for several reasons. The most common are chemical inhomogeneities (macroscopic or/and microscopic), superparamagnetic behaviour due to small crystallite size (<0.1 μm), spin-cluster relaxation, amorphous and spin-glass behaviour. Chemical inhomogeneities may create a narrow distribution of transition temperatures which in turn result in asymmetric broadening and the presence of paramagnetic components in a temperature range very close to T_c. However, the symmetrically broadened Mössbauer lines and the well defined magnetic components for $T < 80$ K do not support the existence of inhomogeneities. The case of superparamagnetic behaviour due to small crystallite size has to be excluded on the basis of the fact that the T_cs determined from Mössbauer spectroscopy and magnetic susceptibility measurements are the same. Similarly, in the case of amorphous or spin-glass magnetic

Table 4. Experimental values of the half-linewidth $\Gamma/2$ in mm s^{-1}, the isomer shift δ relative to that of α-Fe at RT in mm s^{-1}, the quadrupole shift ΔE_Q in mm s^{-1}, the hyperfine magnetic field H in kG and the hyperfine magnetic field spread ΔH modulating the linewidths, as obtained from least-squares fits of the Mössbauer spectra of Fe_2BO_4 below T_c. ΔE_Q denotes the eigenvalues of the Hamiltonian of the quadrupole interaction or of the quadrupole perturbation that are given by the relations $\Delta E_Q = (1/2)e^2qQ(1+\eta^2/3)^{1/2}$ and $\Delta E_Q = (1/4)e^2qQ(3\cos^2\theta - 1)$ for the paramagnetic and the magnetic cases respectively. The asterisks in the table refer to the latter equation for ΔE_Q.

T (K)	Site	δ	ΔE_Q	$\Gamma/2$	H	ΔH	η	θ	ϕ	Area (%)
150	Fe^{3+}	0.51	0.66	0.19	—	—	—	—	—	7
	Fe^{3+}	0.51	0.51	0.19	—	—	—	—	—	7
	Fe^{2+}	1.17	2.00	0.23	—	—	—	—	—	7
	Fe^{2+}	1.17	2.44	0.23	—	—	—	—	—	7
	Fe^{3+}	0.51	−0.07*	0.17	214	24	—	—	—	18
	Fe^{3+}	0.51	0.15*	0.17	223	22	—	—	—	18
	Fe^{2+}	1.17	−2.00	0.17	35	9	0.3	117	349	18
	Fe^{2+}	1.17	2.47	0.17	135	15	0.4	91	339	18
140	Fe^{3+}	0.51	0.68	0.18	—	—	—	—	—	4
	Fe^{3+}	0.51	0.53	0.18	—	—	—	—	—	4
	Fe^{2+}	1.18	2.00	0.22	—	—	—	—	—	4
	Fe^{2+}	1.18	2.47	0.22	—	—	—	—	—	4
	Fe^{3+}	0.51	−0.07*	0.17	328	7	—	—	—	21
	Fe^{3+}	0.51	0.16*	0.17	343	8	—	—	—	21
	Fe^{2+}	1.18	−2.00	0.17	76	1	0.4	115	348	21
	Fe^{2+}	1.18	2.47	0.17	236	4	0.4	93	339	21
80	Fe^{3+}	0.52	−0.04*	0.16	455	—	—	—	—	25
	Fe^{3+}	0.52	0.16*	0.15	480	—	—	—	—	25
	Fe^{2+}	1.20	−2.16	0.19	106	—	0.7	116	350	25
	Fe^{2+}	1.20	2.48	0.16	334	—	0.4	94	347	25
26	Fe^{3+}	0.54	−0.06*	0.15	481	—	—	—	—	25
	Fe^{3+}	0.54	0.15*	0.16	507	—	—	—	—	25
	Fe^{2+}	1.22	−2.18	0.19	114	—	0.8	115	355	25
	Fe^{2+}	1.22	2.48	0.17	358	—	0.4	93	351	25

systems we would expect to observe broad magnetic MS for $T < T_c$, present down to low temperatures ($T/T_c \rightarrow 0$) without any paramagnetic components for $T < T_c$, in contrast with the observed MS. Excluding all of these possibilities, we are left with superparamagnetic relaxation of spin clusters. A model based on vacancies and defects on each magnetic chain can result in spin clusters of various sizes with superparamagnetic behaviour and reproduces the observed spectra. This model is supported by the absence of superlattice peaks in neutron and x-ray diffraction studies [4], which suggests that the charge-ordered domains are small (10–100 Å). Accordingly we simulated the magnetic part of the spectra above 110 K with one magnetic component (sextet) for each of the four sites modulated by a distribution of hyperfine fields (ΔH), plus four paramagnetic components corresponding to those observed above T_c. Representative results of the fits are shown in figure 7 and the fitted parameters are listed in table 4.

4. Conclusions

It is shown by Mössbauer spectroscopy that the Fe_2BO_4 mixed-valence iron oxide at $T < 270$ K has clearly recognizable, localized Fe^{2+} and Fe^{3+} sites. Above this temperature, delocalization starts which spreads throughout the crystal as the temperature increases and is completed at 400 K. This localization–delocalization process is correlated with a charge-order–disorder transition. Localized and delocalized states coexist over a relatively large temperature region. The magnetization and the Mössbauer data reveal magnetic ordering at 155 K and spin-cluster dynamics below this temperature.

Acknowledgments

We are grateful to Dr A Simopoulos for helpful discussions and a critical reading of the manuscript. Thanks are also due to Dr E Devlin and Dr I Panagiotopoulos for fruitful discussions and support in the measurements. Partial support of this work was provided by the PENED-1995 programme from the Greek GSRT and by the 'Georgiou Stayrou' foundation through a scholarship to APD.

References

[1] Attfield J P, Clarke J F and Perkins D A 1992 *Physica* B **180+181** 581
[2] Douvalis A P, Papaefthymiou V, Bakas T and Moukarika A 1997 *Magnetic Hysteresis in Novel Magnetic Materials (NATO ASI Series, vol 338)* ed G C Hadjipanayis (Dordrecht: Kluwer Academic) p 761
[3] Bertaut E F 1950 *Acta Crystallogr.* **3** 473
[4] Attfield J P, Bell A T M, Rodriguez-Martinez L M, Greneche J M, Cernik R J, Clarke J F and Perkins D A 1998 *Nature* **396** 655
[5] Attfield J P, Bell A T M, Rodriguez-Martinez L M, Greneche J M, Retoux R, Leblanc M, Cernik R J, Clarke J F and Perkins D A 1999 *J. Mater. Chem.* **9** 205
[6] Rietveld H M 1969 *J. Appl. Crystallogr.* **2** 65
[7] Coey J M D, Allan J, Xuemin K, Dang N V and Ghose S 1984 *J. Appl. Phys.* **55** 1963
[8] Coey J M D 1984 *Mössbauer Spectroscopy Applied to Inorganic Chemistry* vol 1, ed G J Long (New York: Plenum) p 450
[9] Price D C and Varett F 1983 *Advances in Mössbauer Spectroscopy (Studies in Physical and Theoretical Chemistry vol 25)* ed B V Thosar, J K Srivastava, P K Iyengar and S C Bhargava (Amsterdam: Elsevier Science) p 316
[10] Chechersky V, Nath A, Isaac I, Franck J P, Ghosh K, Ju H and Greene R L 1999 *Phys. Rev.* B **59** 497
[11] Ogale S B, Shreekala R, Bathe R, Date S K, Patil S I, Hannoyer B, Petit F and Marest G 1998 *Phys. Rev.* B **57** 7841
[12] Tkachuk A, Rogacki K, Brown D E, Dabrowski B, Fedro A J, Kimball C W, Pyles B, Xiong X, Rosenman D and Dunlap B D 1998 *Phys. Rev.* B **57** 8509
[13] Leung L K, Morrish A H and Evans B. J 1976 *Phys. Rev.* B **13** 4069
[14] Mørup S, Hendriksen P V and Linderoth S 1995 *Phys. Rev.* B **52** 287